Applied Catalysis B: Environmental 179 (2015) 113–121

Contents lists available at ScienceDirect

Applied Catalysis B: Environmental

journal homepage: www.elsevier.com/locate/apcatb

A PEDOT-coated quantum dot as efficient visible light harvester for photocatalytic hydrogen production

Nagarajan Srinivasan[a], Yuhiro Shiga[a], Daiki Atarashi[a], Etsuo Sakai[a], Masahiro Miyauchi[a,b,*]

[a] Department of Metallurgy and Ceramics Science, Graduate School of Science and Engineering, Tokyo Institute of Technology, 2-12-1 Ookayama, Meguro-ku, Tokyo 152-8552, Japan
[b] Japan Science and Technology Agency (JST), PRESTO, 4-1-8Honcho Kawaguchi, Saitama 332-0012, Japan

ARTICLE INFO

Article history:
Received 6 April 2015
Received in revised form 4 May 2015
Accepted 5 May 2015
Available online 6 May 2015

Keywords:
Quantum dots
Polymer coating
Photo-electrochemistry
Solar energy conversion
Hydrogen production

ABSTRACT

The photocatalytic electrode device comprised of Pt/TiO_2/CdS/CdSe/PEDOT hybrid semiconductors exhibits stable and efficient hydrogen generation through photocatalytic water-splitting reactions. PEDOT polymer was electrochemically coated over a quantum dot-sensitized semiconductor and efficiently suppressed the back electron transfer from the semiconductor, thereby improving the photocurrent as compared to the uncoated control (13 vs 6 mA/cm^2, respectively). Impedance analysis revealed that the PEDOT-coated quantum dot electrode had reduced recombination resistance and increased electron lifetime values. Notably, the prepared electrode showed outstanding performance under visible-light irradiation in the absence of applied bias potential. Under this condition, the hybrid electrode structure generated hydrogen at a rate of 370 μmol cm^{-2} h^{-1} with a sacrificial electrolyte. Furthermore, a quantum efficiency of 6.9% and turnover number of 2210 were achieved by the PEDOT-coated electrode. The photo-stability test revealed that the PEDOT polymer coated electrode showed longer stability compared to the uncoated electrode. The findings presented in this report highlight the advantages of designing and constructing the hybrid electrode structure and be applicable to other photocatalytic materials and photoelectrochemical reactions.

1. Introduction

Hydrogen is a promising energy source for clean and efficient energy applications. Photoelectrochemical hydrogen generation by semiconductors using solar energy has attracted considerable attention in various research fields [1–4]. In particular, methods for the large-scale production of hydrogen from water without the concomitant emission of carbon dioxide are being actively developed [5]. Novel photocatalyst architectures and efficiently designed electrodes that are capable of absorbing the wide range of solar energy spectrum are expected to facilitate photocatalytic water-splitting reactions for the effective hydrogen generation. The water-splitting activities have been investigated on wide-gap semiconductors such as TiO_2 [6] and $SrTiO_3$ [7] under UV light irradiation. Further, the development of visible-light-responsive photocatalysts capable of harvesting a wide range of the solar energy spectrum is highly desirable. The several visible light-responsive semiconductors, including WO_3 [8], Fe_2O_3 [9], $BiVO_4$ [10], $CaFe_2O_4$ [11], and TaON [12], have been successfully constructed for water splitting applications.

Numerous reports during the past four decades have demonstrated the usefulness of metal chalcogenides quantum dots (CdTe [13], PbS [14], CdS [15], and CdSe [15]) for solar-driven water splitting owing to their narrow visible-light responsive band gap and high absorption coefficient [16]. These studies reported the efficient short circuit photocurrent [17] and enhanced photo electrochemical reactions [18]. However, because of the inevitable photodegradation of quantum dots in aqueous medium, metal chalcogenide quantum dots are generally considered to be unsuitable for solar-driven water-splitting applications. Although passivation layer coating has been reported to prevent the degradation of quantum dots [15], such systems suffer from a lack of long-term stability, which is critical for the commercial viability as a photocatalytic semiconductor. In addition to the stability, electrode structure is very important for the development of quantum

* Corresponding author at: Department of Metallurgy and Ceramics Science, Graduate School of Science and Engineering, Tokyo Institute of Technology, 2-12-1 Ookayama, Meguro-ku, Tokyo 152-8552, Japan. Tel.: +81 3 5734 2527; fax: +81 3 5734 3368.
E-mail address: mmiyauchi@ceram.titech.ac.jp (M. Miyauchi).

http://dx.doi.org/10.1016/j.apcatb.2015.05.007
0926-3373/

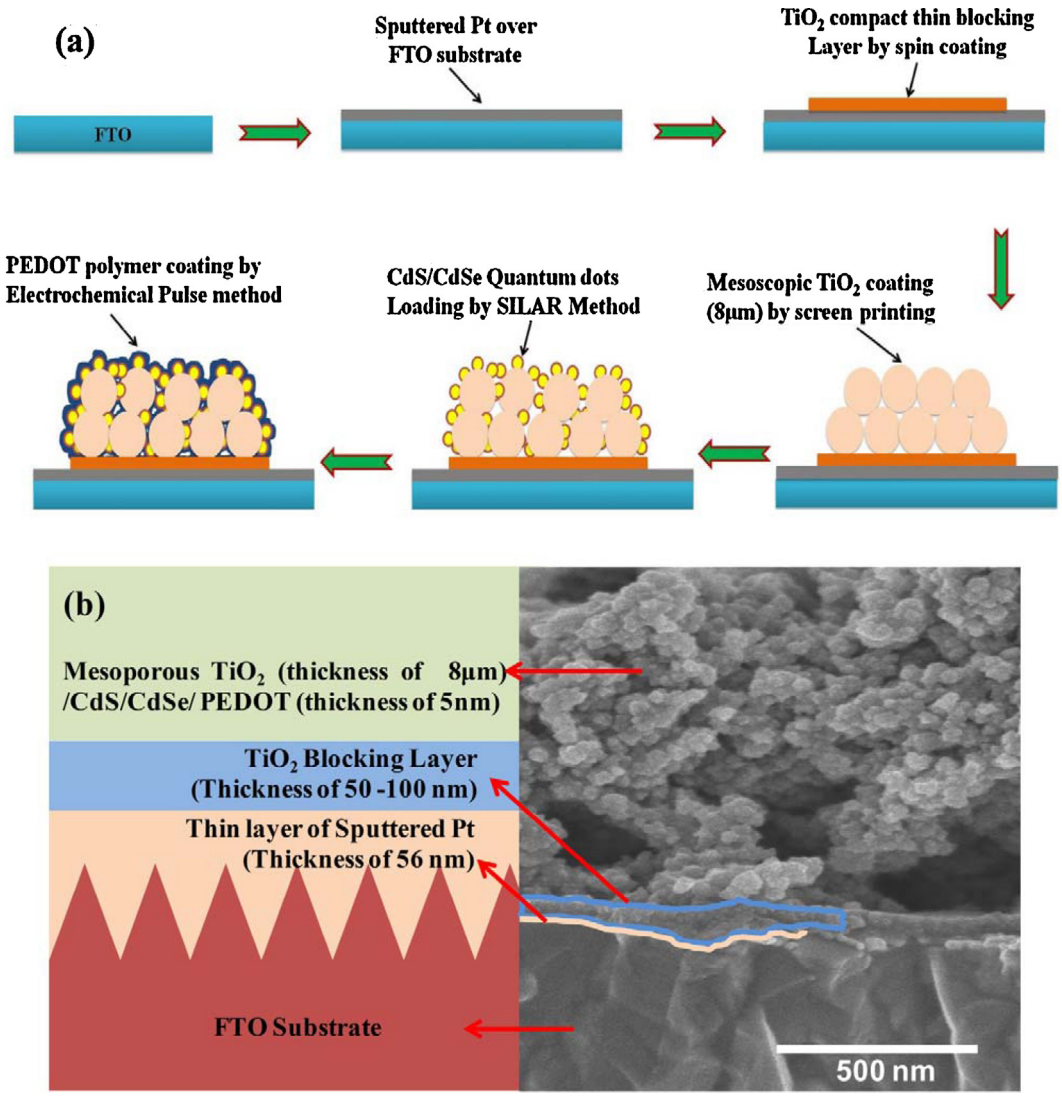

Fig. 1. (a) Structural illustration of electrode construction and (b) Cross section SEM image with respect to electrode Architecture.

dots based solar water splitting. Recently the quasi artificial leaf electrode structure based on PbS quantum dots [19] and dihydrolipolic acid as a capping agent to stabilize the light absorbing QDs (CdSe) for hydrogen evolution reaction were demonstrated [20]. These results indicate that quantum dot-based photoelectrode does not require layered p-n junction films like silicon solar cells, as photo-generated electrons and holes are efficiently separated at the interface between the quantum dots and mesoporous medium. The development of improved coating methods for quantum dots and more efficient electrode designs are necessary for highly photo stable systems that are suitable for practical application.

Herein, we establish a new design for efficient quantum dot based water-splitting systems with long-term stability. We have focused on the hole-conducting polymer poly (3,4-ethylenedioxythiophene) (PEDOT), which has electrochemical stability [21] and excellent electrocatalytic activity [22,23], as a material to inhibit the photo-degradation of CdS/CdSe quantum dots. The key feature of this approach is the use of PEDOT to synergistically prevent photo-degradation of the CdS/CdSe (QDs) surface and to efficiently transport photogenerated holes to promote the desired hole-scavenging reactions. PEDOT allows the effective separation of photogenerated electrons and holes without any bias potential or solid state layered p-n junction like an expensive silicon solar cell. In the present report, we attempt to construct a robust electrode structure in aqueous solution and achieve efficient hydrogen generation under visible-light irradiation with a sacrificial electrolyte.

2. Experimental section

2.1. Materials

All of the reagent grade materials are procured from Kanto Chemicals & Biological, Japan and were used for electrode preparation without further purification.

2.2. Electrode preparation

Mesoporous TiO_2 film of 8 μm thickness was prepared by screen-printing using commercial (P25) TiO_2 nanoparticle paste onto the FTO glass substrates, followed by annealing at 500° C for 1 h. Prior to TiO_2 nanoparticle coating, the FTO substrates were coated by a compact thin layer of TiO_2 (50 nm) by spin coating method using titanium isopropoxide as a precursor material. The CdS and CdSe quantum dots sensitized onto a TiO_2 electrodes by a successive ionic layer adsorption and reaction (SILAR) method.

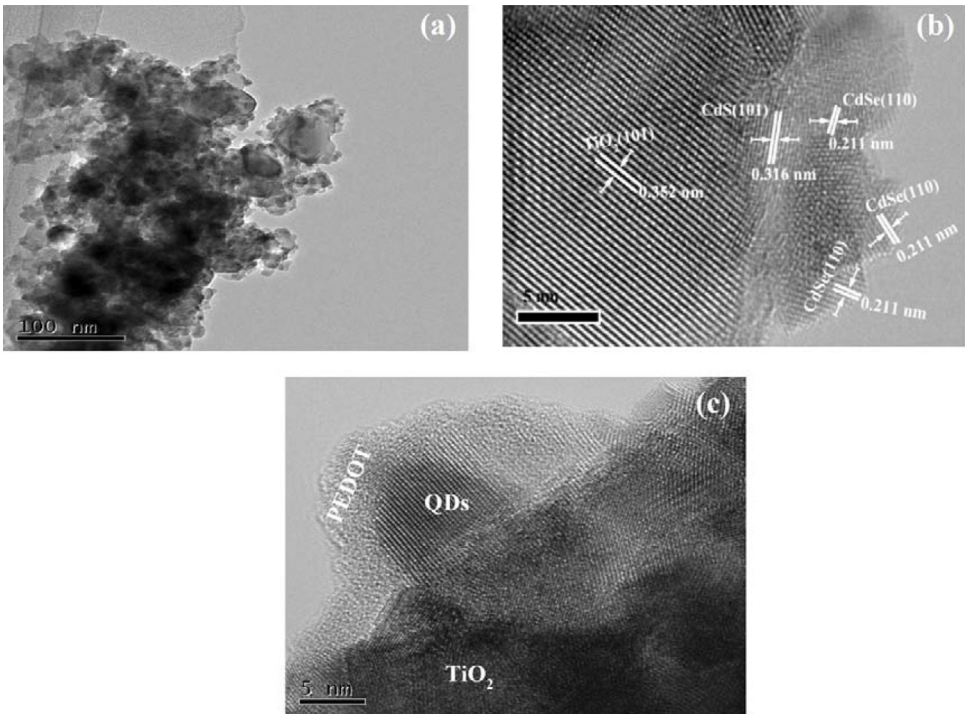

Fig. 2. (a) Low magnification TEM images showing a mesoporous structure of the TiO_2/QDs, (b) HRTEM fringes pattern corresponds to the arrangement of CdSe and CdS quantum dots over TiO_2 and (c) PEDOT polymer coated over TiO_2/QDs.

This SILAR method was similar to the procedure described in the previous papers [1,2]. A TiO_2 electrode was immersed into a 0.5 M $Cd(NO_3)_2$ ethanol solution for 5 min, washed with ethanol, and then immersed for another 5 min into a 0.5 M Na_2S methanol solution and washed with methanol. This two-step immersion procedure is termed as one SILAR cycle, and the crystallite growth of CdS were controlled by repeating the SILAR cycles. For CdSe quantum dots preparation, the sodium selenosulphate (Na_2SeSO_3) is used as the Se source and preparation of Na_2SeSO_3 aqueous solution was followed by reported papers [15,24]. The CdSe quantum dots sensitization is resembled to that of CdS sensitization, except the immersion time (1 h) and constant temperature of 60° C should be maintain during electrode immersion in Na_2SeSO_3 solution and Na_2S solution. The SILAR cycles of CdS (5 cycles) and CdSe (3 cycles) quantum dots were optimized.

2.3. Electropolymerization of PEDOT polymer

The PEDOT polymer coated over TiO_2/QDs electrodes were fabricated by an electropolymerization of EDOT (3,4-ethylenedioxythiophene) on QDs/TiO_2 electrode substrates using $LiClO_4$ as supporting electrolytes, and acetonitrile as a solvent. The PEDOT concentration was 1×10^{-3} M, and the three-electrode cell was used for electropolymerization of PEDOT, where TiO_2/QDs as working electrode, and saturated Ag/AgCl and platinum foil were used as reference and counter electrodes, respectively. The electropolymerization was carried out under room temperature in nitrogen atmosphere by purging the nitrogen gas which removes the dissolved oxygen from the electrolyte solution. The electropolymerization was performed using pulse current method [26], the anodic pulse current (5 mA to 10 mA) and cathodic pulse current (−3 mA to −7 mA) was adjusted and optimized with the electrode surface area. A second of anodic pulse, followed by another 1 s of cathodic pulse, and 5 s of zero current were applied (see our supplementary information, Fig. S1). This above procedure is termed as one pulse cycle. To increase the PEDOT polymer coating thickness over TiO_2/QDs electrode pulse cycles were repeated.

2.4. Characterization and photoelectrochemical measurement

The morphology of the materials was observed using a transmission electron microscopy (TEM, JEM-2010F, JEOL Ltd. Japan.). EDX measurement was carried out by using Keyence VE 9800 SEM Microscope coupled with EDAX Genesis unit. The absorption spectra of the photoelectrode were measured on a UV–visible (UV–vis) spectrophotometer (V-660, JASCO Ltd.) equipped with an integration sphere unit using diffuse reflection mode. The FTIR spectra were recorded by using Model IR-6100 apparatus (JASCO Ltd.).

The photoelectrochemical experiments were carried out using potentiostat/galvanostat (HZ-5000, Hokuto Denko Ltd.). The photocurrent density voltage (I-V) curve, electrochemical impedance spectroscopy and open circuit voltage decay measurements were carried out using three electrode systems, where the TiO_2/CdS/CdSe/PEDOT working electrode, Pt plate as counter electrode and a saturated Ag/AgCl was used as the reference electrode. The electrolyte solution containing 0.24 M Na_2S and 0.34 M Na_2SO_3 was used as sacrificial hole scavenger. A 150 W Xe lamp was used as the light source. The light was passed through a 430 nm optical UV cutoff filter, which pass out the wavelengths longer than 430 nm to illuminate the photoanode. The I-V curves were scanned for three times, and the average photocurrent densities for each scan were plotted. A frequency response analyzer (FRA) was used for EIS measurements using amplitude of 10 mV over a frequency range from 40 kHz to 1 mHz. The incident photon to current conversion efficiency (IPCE) measurement system was calibrated by silicon photodiode reference cell and the IPCE spectra were measured as function of wavelength from 400 to 800 nm at 0 bias voltages with a CEP-99W system (BUNKOH-KEIKI Co., Ltd. Japan).

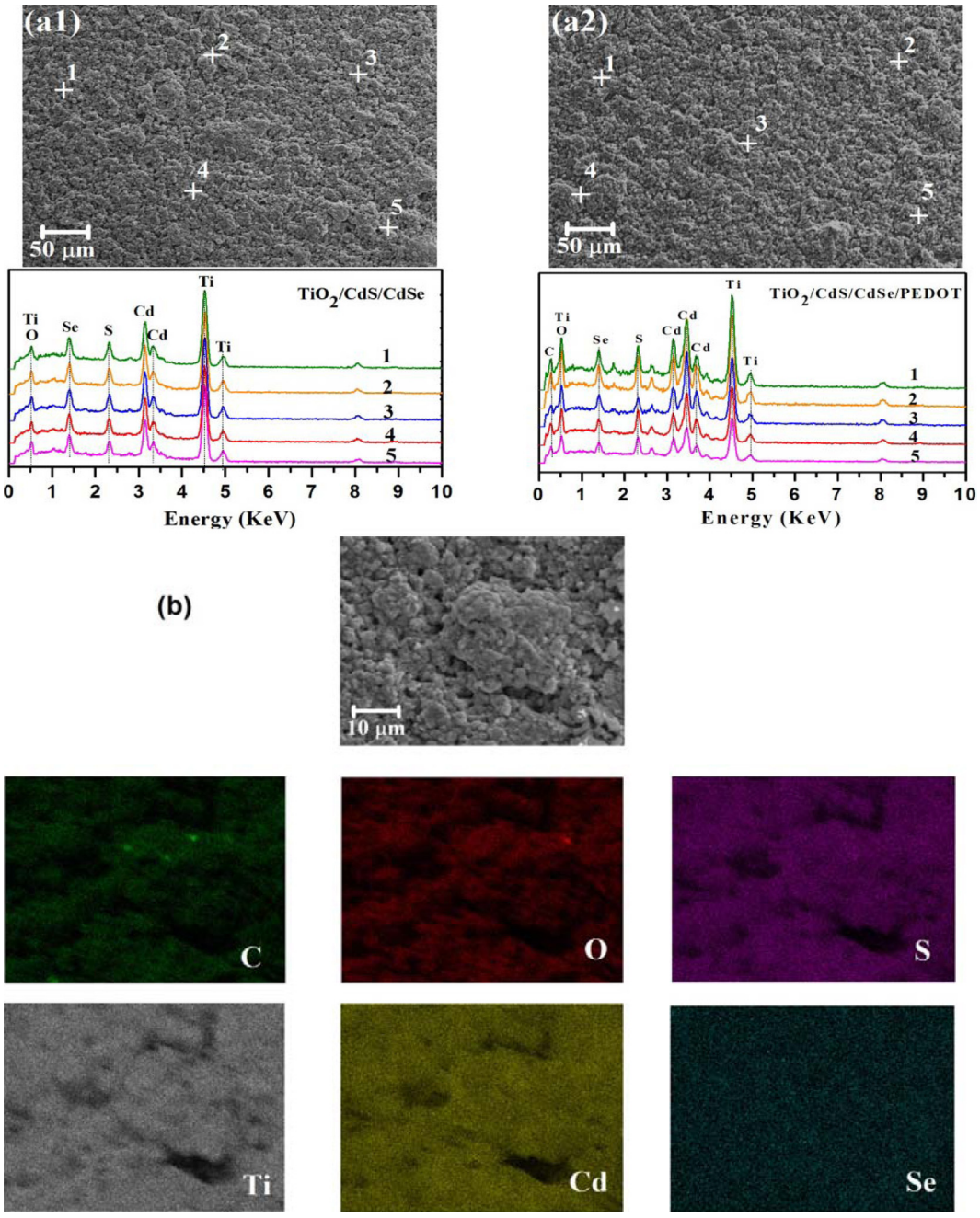

Fig. 3. The EDX spot analysis of (a1)TiO_2/QDs, (a2)TiO_2/QDs/PEDOT and (b) EDX elemental mapping of TiO_2/QDs/PEDOT.

The IPCE of the samples was calculated from the Eq. (1) as follows [25]

$$\text{IPCE}(\%) = \frac{1240 \times J[\mu\text{A/cm}^2]}{\lambda \times P[\mu\text{W/cm}^2]} \times 100 \quad (1)$$

where J is the photocurrent density generated by monochromatic light with wavelength λ and intensity of Photon flux (P). Photon flux was determined by using a standard silicon solar cell.

2.5. Photocatalytic hydrogen production

In contrast to the photoelectrochemical measurement on a conventional two electrodes system, a novel Pt/TiO_2/CdS/CdSe/PEDOT wire free, efficient, single hybrid electrode system was designed and fabricated for photocatalytic hydrogen production. In this electrode design, Pt nanoparticles were firstly deposited over an FTO glass substrate by magnetron sputtering, followed by compact thin TiO_2 layer, mesoscopic porous TiO_2 layer, QDs and PEDOT polymer coating. The detailed experimental fabrication scheme of the hybrid electrode and the SEM cross section images of the fabricated electrode are shown in Fig. 1. H_2 evolution was measured by using closed gas-circulating system connected to a gas chromatogram. The FTO/Pt/TiO_2/QDS/PEDOT electrode area of 4 cm^2 was placed in aqueous solution containing 0.24 M Na_2S and 0.34 M Na_2SO_3 acting as sacrificial electrolyte contained in a Pyrex glass beaker. The electrolyte solution and headspace were purged with argon gas and the cell was illuminated with a light source of 150 W Xe lamp with 430 nm cutoff filter. The evolved H_2 gas was detected by on-line gas chromatography (Shimadzu Co., TCD, 5 Å molecular sieves, Ar

carrier gas). The amounts of generated H_2 gas collected up to 6 h under light illumination were converted in to μmol for calculations.

3. Result and discussion

TEM images of the TiO_2/QDs and PEDOT polymer-coated TiO_2/QDs are shown in Fig. 2. The size of QDs particles were ranged from 5 to 10 nm in diameter (Fig. 2 (a)). The TEM lattice fringe spacing proved that the CdS crystallite deposited on TiO_2 and CdSe crystallite located at the surface of CdS (Fig. 2(b)). From the Fig. 2 (c) the PEDOT polymer coating layer was found to be approximately 2–5 nm in thickness and it uniformly covered the surface of the QDs and TiO_2 semiconductor. The EDX elemental spot analysis were performed on with and without PEDOT polymer coated electrodes and the results are shown in Fig. 3(a1) and 3(a2). The spot analysis results showed the elements like Cd, S, Se, Ti and O which confirms the presence of CdS, CdSe and TiO_2 semiconductor. In addition, the Fig. 3(a2) showed the elemental peak of carbon (C) which corresponds to presence of PEDOT polymer coating over the semiconductor. The PEDOT coatings further probed by EDX mapping analysis are shown in Fig. 3(b). The mapping results clearly revealed that the PEDOT polymer was uniformly coated over QDs/TiO_2 semiconductor surface.

In addition, PEDOT polymer coating over TiO_2/QDs was confirmed by using FTIR analyses which are shown in Fig. 4. The peaks at about 1525 and 1480 cm^{-1} are associated with C=C asymmetric stretching vibration. The peak at 1360 cm^{-1} corresponds to C—C and C=C stretches of the thiophene ring. The peaks at about 1150 and 1105 cm^{-1} are assigned to the C—O—C band stretching vibration. The peak at about 980 cm^{-1} can be assigned to the C—S stretching vibration. All the peaks obtained can be attributed to the predominant role of PEDOT over the prepared electrode, indicating that PEDOT was successfully electrodeposited over TiO_2/QDs electrode. The FTIR spectrum of synthesized PEDOT electrode was roughly consistent with reported literatures [27–29]

Fig. 5 shows photo-current density versus bias potential for the TiO_2/QDs electrodes coated with different thicknesses of PEDOT. In this photo-electrochemical experiment, a Pt substrate was used as a counter electrode for hydrogen generation and 0.24 M Na_2S and 0.34 M Na_2SO_3 (pH 12) acting as sacrificial electrolyte. The pure TiO_2 and PEDOT electrodes did not generate photocurrent under visible light irradiation. We also performed I-V curve

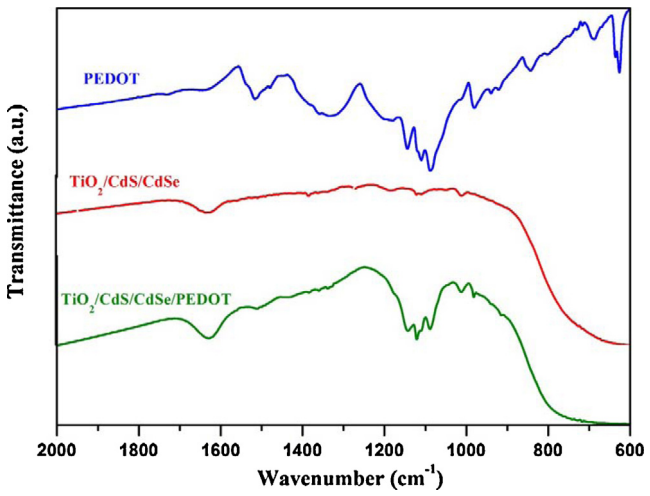

Fig. 4. FTIR spectra of PEDOT, TiO_2/QDs, and TiO_2/QDs/PEDOT electrodes.

measurement under dark conditions (Supplementary Information S2), and all electrodes in the present study did not generate any current under dark condition. Under the light irradiation, it is noted that the PEDOT-coated TiO_2/QDs electrodes showed higher photocurrent density values as compared to uncoated TiO_2/QDs electrodes like TiO_2/CdS, TiO_2/CdSe and TiO_2/CdSe/CdS. Although the UV–vis spectra for TiO_2/QDs/PEDOT electrodes (Fig. 6) revealed that the PEDOT exhibited small inherent absorption from visible to infrared light, the action spectra of incident photon to current conversion efficiency (IPCE) exhibited the same spectra between the sample with PEDOT coating and that without PEDOT polymer (Fig. 7). These results indicate that the inherent PEDOT absorption does not contribute the photocurrent generation. In the TiO_2/QDs/PEDOT system, the excited electrons are injected into the conduction band of TiO_2 and subsequently migrate to the FTO layer, whereas the photogenerated holes react with the sacrificial agent through the PEDOT layer. The significant increase in current density exhibited by the PEDOT-coated electrodes can be ascribed to the effective charge separation between the QDs semiconductor and the electrolyte, a property that promoted efficient electron transfer to the counter electrode through the avoidance of recombination. However, further increases in the thickness of the PEDOT layer

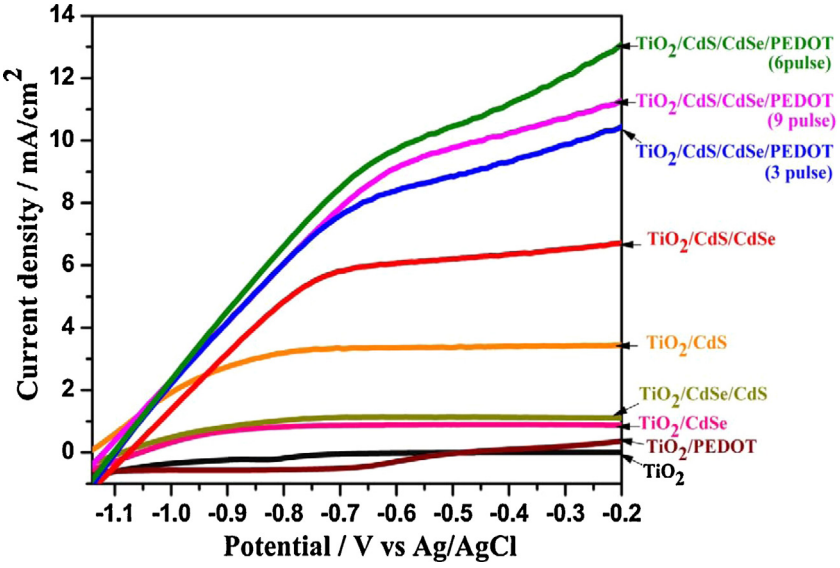

Fig. 5. Current density versus potential curve measured for different photoelectrode. (Legend shows order of CdS and CdSe coated over mesoporous TiO_2).

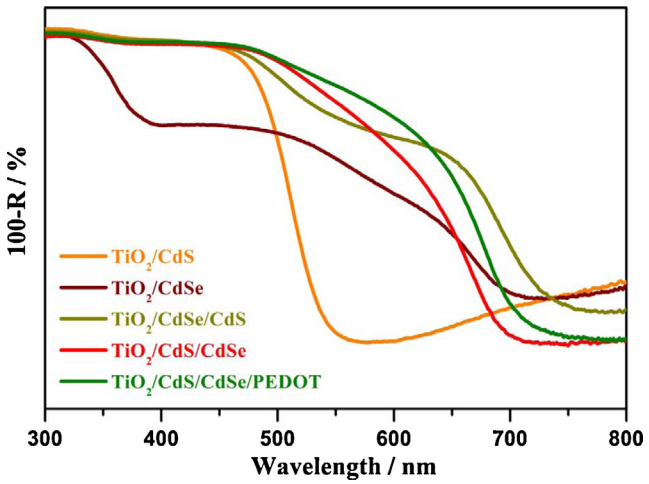

Fig. 6. UV–vis absorption spectra of the different quantum dotelectrode measured in reflectance mode.

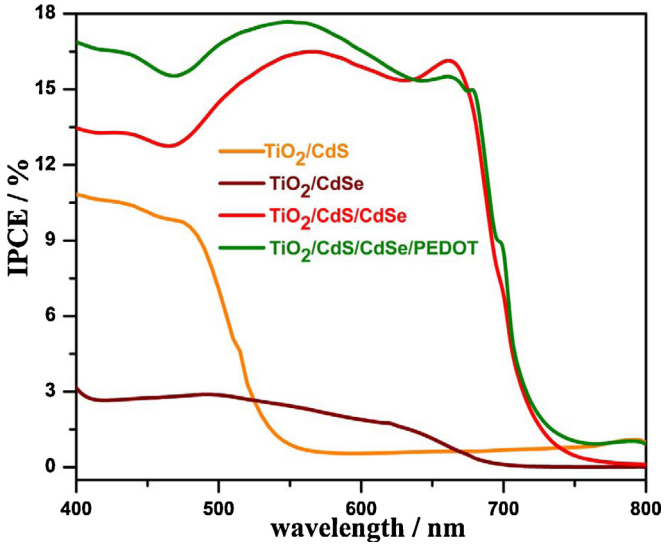

Fig. 7. Incident photon to current conversion efficiencies (IPCE) for various electrodes was measured by recording the short circuit photocurrents at different excitation wavelengths. The measurement was carried out in two electrode system with 0 V bias potential.

tended to reduce the current density due to impairment or insulation of the hole mobility. At the optimized thickness of the PEDOT (6 pulse times) coating, the TiO_2/QDs/PEDOT electrodes exhibited a current density value of 13 mA/cm^2 at −0.2 V vs Ag/AgCl.

In addition to the effect of PEDOT coating, we observed the dependence of the coating order of QDs on the photocurrent properties. The photocurrent density of TiO_2/CdS/CdSe electrode was higher than that of TiO_2/CdSe/CdS electrode and these results indicated the stepwise band edge formation followed by the alignment of Fermi level at CdS/CdSe interface [15] Our IPCE measurement (Fig. 7) also revealed that those of TiO_2/CdS and TiO_2/CdSe electrodes were 10% and 3%. The higher IPCE% value for TiO_2/CdS electrode indicated that the electron hole pair's separation and collection are efficiently taking place due to the interface between CdS and TiO_2 has better junction and closer work function matching than that between CdSe and TiO_2. The PEDOT polymer coated TiO_2/CdS/CdSe electrode showed efficient IPCE value (17.5%) because its photoactive region extends up to 700 nm with efficient charge separation by the band alignment of semiconductors QDs and PEDOT polymer.

Further, the electron transport kinetics was investigated by an impedance spectroscopy (Fig. 8). The EIS spectrums were ana-

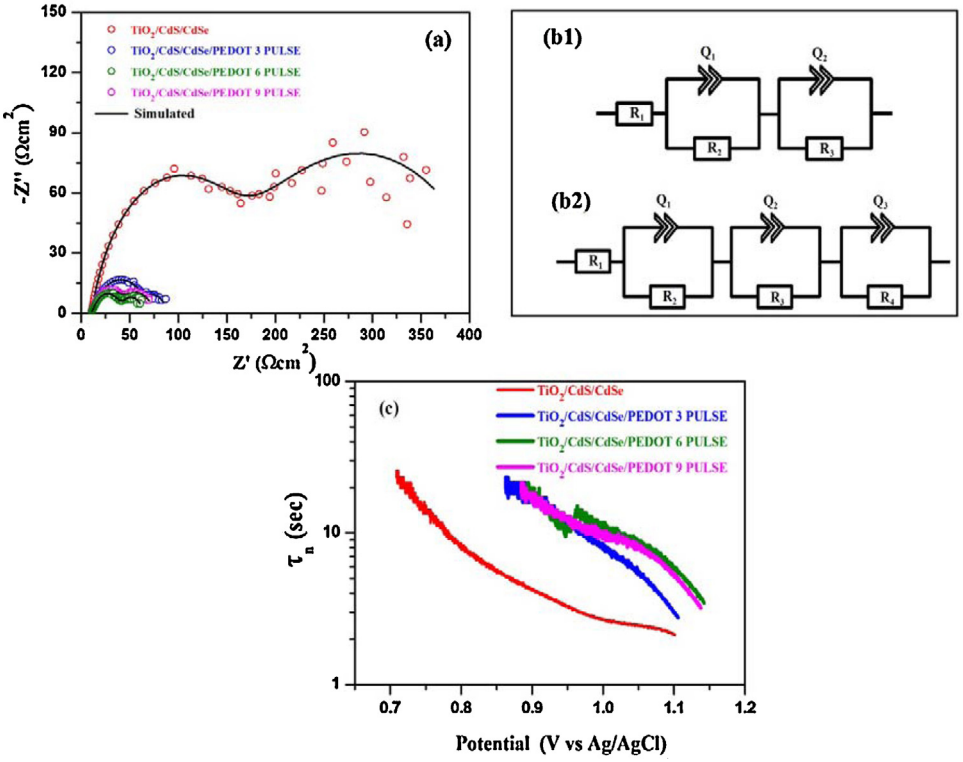

Fig. 8. (a) Nyquist plots measured for different quantum dot electrodes at −0.5 V vs Ag/AgCl in 0.24 M Na_2S and 0.34 M Na_2SO_3 electrolyte. (Bullets are experimental data and the solid line represents fitted data), (b) The corresponding fitted equivalent circuit model and (c) Electron lifetime as a function of open circuit voltage (V_{oc}) derived from the V_{oc} decay for different electrodes.

lyzed and were fitted with appropriate equivalent circuit model. Fig. 8(a) shows the Nyquist plot of the samples with and without PEDOT polymer coating. The presence of two semicircles in the uncoated sample can corresponds to the Pt counter electrode/electrolyte and TiO_2/QDs/electrolyte interface. However, in case of PEDOT coated electrode, the presence of a third additional semicircle can be attributed to the interaction between PEDOT polymer layer and ions present in the electrolyte solution. Fig. 8(b1) shows the fitted equivalent circuit obtained for electrode without polymer coating as R_1 (R_2Q_1) (R_3Q_2) where, solution resistance (R_1), charge transfer resistance and double layer capacitance of Pt counter electrode (R_2, Q_1) and TiO_2/QDs (R_3, Q_2) form the major components of the circuit. While Fig. 8(b2) represents the equivalent circuit as R_1 (R_2Q_1) (R_3Q_2) (R_4Q_3) for the PEDOT polymer coated TiO_2/QDs electrode. In this case of R_4 and Q_3 represent the charge transfer resistance and double layer capacitance of the PEDOT polymer coated layer with electrolyte. The fitted equivalent circuits data for electrode without polymer coating showed higher charge transfer resistance values which indicate that the acceptability of electron recombination as the most difficult reaction taking place on the photoelectrode surface [30]. All three PEDOT polymer coated electrode show lower charge transfer resistance, which reveals that PEDOT polymer facilitate holes separation and effective blocking of the electron from the recombination process [31]. Further, the EIS analysis data corroborate well with the I–V results.

In addition, the electron lifetime (τ_n), as determined by the decay time with respect to the open circuit voltage (V_{oc}) which are shown in Fig. 8(c). The voltage-recombination lifetime was calculated from the Eq. (2) as follows, [32,33]

$$\tau_n = -\frac{k_B T}{e}\left(\frac{dV_{oc}}{dt}\right)^{-1} \quad (2)$$

where k_B is Boltzmann's constant, T is the temperature, V_{oc} is the open circuit voltage, and e is the elementary charge. The Fig. 8(c) revealed that the V_{oc} decay rate for the TiO_2/QDs electrode decreased rapidly as compared to that of the PEDOT-coated electrode. The calculated electron lifetime of the PEDOT-coated TiO_2/QDs electrode was markedly higher than that of the TiO_2/QDs electrode, indicating that the PEDOT polymer coating efficiently

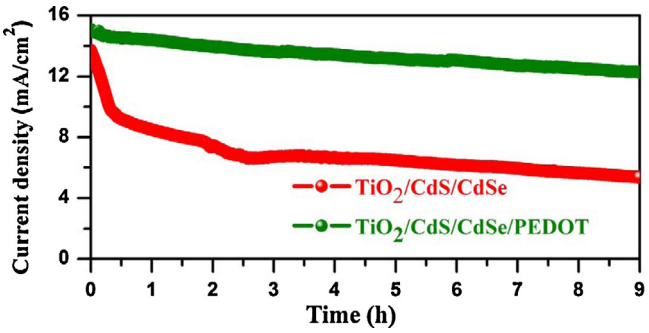

Fig. 9. Photo stability of TiO_2/QDs and TiO_2/QDs/PEDOT electrode measured by photocurrent over time in 0.34 M Na_2SO_3, 0.24 M Na_2S electrolyte solution with applied bias potential of 0 V vs Ag/AgCl under visible light illumination from a 150 W Xe lamp equipped with an UV cut-off filter below 430 nm.

enhances charge transport and reduces recombination of electron-hole pairs.

The stability of the PEDOT-coated TiO_2/QDs electrode photocurrent over time in the presence of a sulfur sacrificial agent, under illumination with >420 nm light is in shown Fig. 9. The initial photocurrent density of TiO_2/QDs was slightly lower than that of TiO_2/QDs/PEDOT because of charge carrier recombination of QDs without PEDOT coating [34]. After 9 h of continuous illumination, the photocurrent density of TiO_2/QDs electrodes had markedly deteriorated. However, in the case of the PEDOT-coated TiO_2/QDs electrode, the initial photocurrent was one-fold higher compared to the uncoated electrode and the current density was highly stable for 9 h. The photostability of PEDOT-coated TiO_2/QDs electrode was highest among the reported QD semiconductors electrode for photo-electrochemical water splitting [18,35–37]. The PEDOT coating increased the stability of the photocurrent by accepting photogenerated holes from QDs, thereby effectively inhibiting the oxidative degradation of QDs. PEDOT is an effective organic hole conductor in light-emitting diodes and organic solar cells [38], and is extremely stable in the presence of water or oxygen molecules as compared to uncoated QDs. The present results indicate that PEDOT-coated TiO_2/QDs electrodes retain their stability during water-splitting reactions.

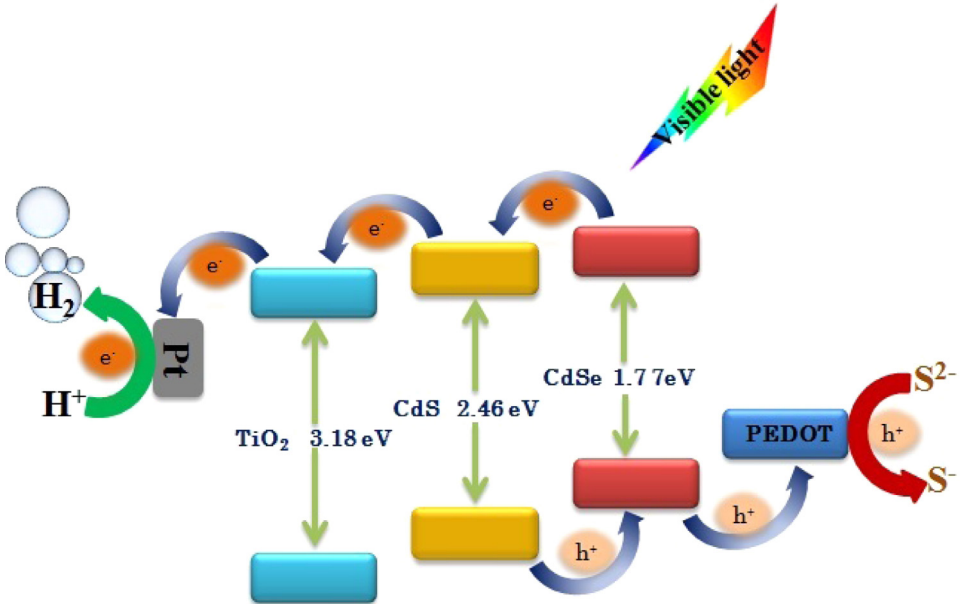

Fig. 10. Schematic illustration of electronic band structure and the respective photogenerated charge transfer mechanism for hydrogen generation in Pt/TiO_2/QDs/PEDOT electrode.

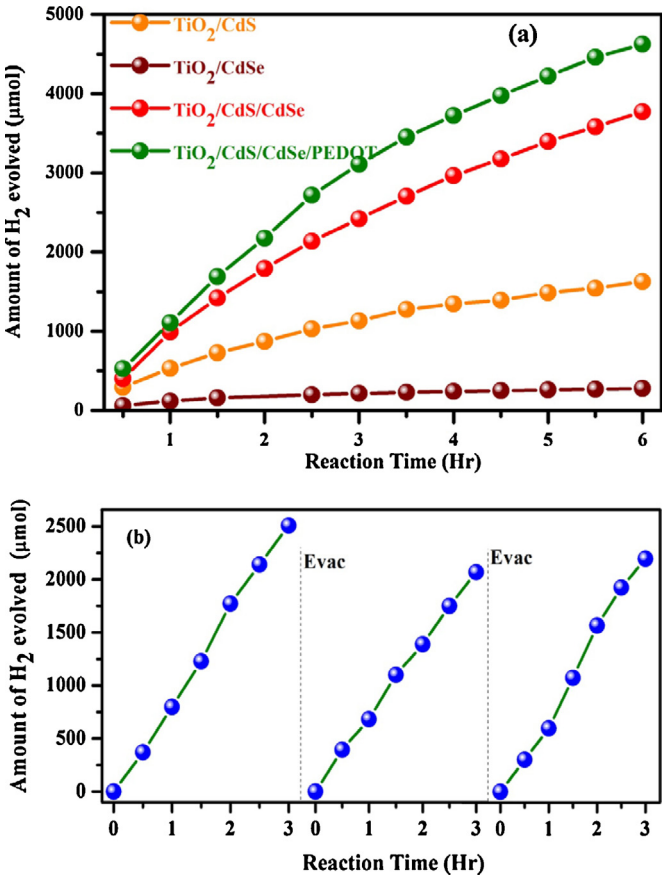

Fig. 11. (a) Photocatalytic hydrogen evolution from TiO_2/CdS, TiO_2/CdSe,TiO_2/QDS and PEDOT coated TiO_2/QDS electrodes. (b) Time course of photocatalytic hydrogen evolution for PEDOT coated TiO_2 /QDS electrode (surface area of 4 cm^2) in 0.34 M Na_2SO_3, 0.24 M Na_2S electrolyte solution under visible light illumination from a 150 W Xe lamp equipped with an UV cut-off filter below 430 nm.

For photocatalytic hydrogen evolution reaction, the modification of a semiconductor with co-catalyst such as platinum (Pt) nanoparticles is generally required for the multi-electron reduction to generate hydrogen molecules (H_2). In addition, previous studies have reported utilizing wire contacts between separated photoanodes and Pt electrodes to generate H_2 [39]. To overcome these problems of complicated electrode structures with additional exoergic bias application, we developed a novel wire-free electrode for efficient H_2 generation without any bias potential (see our detailed preparation scheme and SEM cross-sectional images shown in Fig. 1). On the basis of our spectroscopic and photo-electrochemical results mentioned above, the expected electric structure and charge transfer reactions of the TiO_2/QDs/PEDOT electrode for hydrogen generation are shown in Fig. 10. The prepared wire free electrode was immersed in sacrificial sulfur electrolyte and exposed to visible-light illumination. Under these conditions, photogenerated electrons would be rapidly transferred from QDs to TiO_2 and would also be injected into Pt active centers, resulting in H_2 generation. The porous nature of the electrode is critical for H_2 production activity, as protons in aqueous solution efficiently diffuse from the surface to the underlying Pt layer. Simultaneously, the photogenerated holes extracted from the PEDOT polymer traverse through the electrolyte for oxidation reactions.

The hydrogen generation properties of PEDOT-coated and uncoated electrodes were shown in Fig. 11(a). The obtained results confirmed that the PEDOT-coated electrode exhibited a higher generation rate than the latter. These trends were similar to the photocurrent results. It is noteworthy that the hydrogen generation rate of the uncoated TiO_2/QDs electrode decreased as a result of photodegradation. In contrast, the hydrogen generation rate of the PEDOT-coated TiO_2/QDs electrode was relatively constant for the first 3 h, but then gradually deceased at a similar rate to the uncoated electrode, as shown in Fig. 11(a). This behavior can be ascribed to the consumption of the sacrificial sulfur electrolyte through hole scavenging reactions. Finally, the calculated hydrogen evolution rate from the PEDOT polymer-coated electrode under visible-light irradiation reached 1.1 mmol/cm^2 (6 h). The hydrogen generation rates of these electrodes were measured when we evacuated gas phase reactor and added the sacrificial agent in the electrolyte (Fig. 11(b)). These results further demonstrate the stability and reproducibility of the PEDOT-coated TiO_2/QDs electrode for water splitting.

On the basis of our hydrogen generation value for the PEDOT-coated TiO_2/QDs electrode (1.1 mmol/cm^2 over 6 h), the quantum efficiency and turnover numbers were calculated using the following Eqs (3) and (4), [3,40–42]

$$\text{Internal Quantum Efficiency}\,(\varphi) = \frac{\text{Number of reacted electrons}}{\int_{300}^{800} \text{Number of absorbed photons.d}\lambda}$$

$$\times 100 = \frac{\text{Numbered of evolved hydrogen molecules x2}}{\int_{300}^{800} \text{Number of absorbed photons.d}\lambda} \times 100 \qquad (3)$$

Here the number of evolved H_2 molecules (moles/cm^2/sec) was quantified and we considered the two electron transfer mechanism for the generation of one molecule of H_2. It was assumed that all incident photons were absorbed by the reaction system. The corresponding absorption values measured form UV–vis reflectance of QDs and the light spectrum of Xe lamp from 300 nm to 800 nm was recorded by radiometer, we estimated the number of absorbed photon numbers.

$$\text{Turn Over Number}\,(\text{TON}) = \frac{\text{Number of reacted Photoelectrons}}{\text{Amount of Photocatalyst}}$$

$$= \frac{\text{Molar quantity of evolved hydrogen molecules} \times 2}{\text{Molar quantity of Photocatalyst}} \qquad (4)$$

The turnover number is defined as the number of a product divided by the number of active sites on catalyst surface. Generally, active sites in heterogeneous photocatalyst (our electrode system CdS/CdSe quantum dots) are difficult to quantify. Here, we considered that the total molar quantity of the catalyst as the number of active sites [3]. So carefully measuring the weight of the electrodes before and after CdS, CdSe coating, the loaded CdS and CdSe quantum dots final weights were evaluated. From the calculated weights, amount of QDs are estimated at 2.07×10^{-6} M (CdS) and 2.09×10^{-6}M (CdSe), respectively.

The calculated quantum efficiency of the reaction was 6.9% and the turn over number (TON) was greater than 2200. To our knowledge, these values are the highest reported to date among QD semiconductors electrode for photo-electrochemical water splitting under visible-light illumination [43]. Further, the TON was calculated with respect to the hydrogen evolution interval time and the results are given in Table (Supplementary Information T1). The PEDOT-coated TiO_2/QDs electrode showed higher TON as compared to that of TiO_2/QDs electrode without PEDOT. Currently, we are working for more effective materials and electrode structures, such as the Z-scheme, for complete water splitting based on the promising system comprised of QD and PEDOT described here.

4. Conclusion

The PEDOT polymer-coated TiO_2/QDs electrodes showed enhanced photo-stability and increased photocurrent due to

reduced photo-degradation and efficient charge transfer. Based on the Pt/TiO_2/QDs/PEDOT hetero-structure, we designed a unique electrode structure that displayed the highest hydrogen generation rate among QD semiconductors reported to date and large turnover numbers in sacrificial sulfur electrolyte under visible-light illumination. The newly designed electrode structure may be applicable to other photocatalytic materials and photoelectrochemical reactions.

Acknowledgements

This work is supported by JST, PREST, Japan. The authors thank the Japan Society for the Promotion of Science (JSPS) for support through a JSPS fellowship. We also thank Mr. A. Genseki at the Center for Advanced Materials Analysis in Tokyo Institute of Technology for help with the TEM observation, and also acknowledge Mr. Greg Newton for the critical reading of the manuscript.

Appendix A. Supplementary data

Supplementary data associated with this article can be found, in the online version, at http://dx.doi.org/10.1016/j.apcatb.2015.05.007

References

[1] M.G. Walter, E.L. Warren, J.R. McKone, S.W. Boettcher, Q.X. Mi, E.A. Santori, N.S. Lewis, Chem. Rev. 110 (2010) 6446–6473.
[2] K. Maeda, K. Domen, J. Phys. Chem. Lett. 1 (2010) 2655–2661.
[3] A. Kudo, Y. Miseki, Chem. Soc. Rev. 38 (2009) 253–258.
[4] R. Abe, J. Photochem. Photobiol. C 11 (2010) 179–209.
[5] A.J. Esswein, D.G. Nocera, Chem. Rev. 107 (2007) 4022–4047.
[6] K. Nakata, A. Fujishima, J. Photochem. Photobiol. C 13 (2012) 169–189.
[7] R. Konta, T. Ishii, H. Kato, A. Kudo, J. Phys. Chem. B. 108 (2004) 8992–8995.
[8] C. Santato, M. Ulmann, J. Augustynski, Adv. Mater. 13 (2001) 511–514.
[9] A. Kay, I. Cesar, M.J. Gratzel, J. Am. Chem. Soc. 128 (2006) 15714–15721.
[10] K. Sayama, A. Nomura, T. Arai, T. Sugita, R. Abe, M. Yanagida, T. Oi, Y. Iwasaki, Y. Abe, H. Sugihara, J. Phys. Chem. B 110 (2006) 11352–11360.
[11] S. Ida, K. Yamada, T. Matsunaga, H. Hagiwara, Y. Matsumoto, T.J. Ishihara, J. Am. Chem. Soc. 132 (2010) 17343–17345.
[12] G. Hitoki, T. Takata, J.N. Kondo, M. Hara, H. Kobayashi, K. Domen, Chem. Commun. 16 (2002) 1698–1699.
[13] H.M. Chen, C.K. Chen, Y.C. Chang, C.W. Tsai, R.S. Liu, S.F. Hu, W.S. Chang, K.H. Chen, Angew. Chem. Int. Ed. 49 (2010) 5966–5969.
[14] Y. Jin-nouchi, T. Hattori, Y. Sumida, M. Fujishima, H. Tada, Chem. Phys. Chem. 11 (2010) 3592–3595.
[15] Y.L. Lee, C.F. Chi, S.Y. Liau, Chem. Mater. 22 (2010) 922–927.
[16] K. Zhang, L.J. Guo, Catal. Sci. Technol. 3 (2013) 1672–1690.
[17] K. Kim, M.J. Kim, S.I. Kim, J.H. Jang, Sci. Rep. -U.K. 3 (2013) 3330.
[18] P. Rodenas, T. Song, P. Sudhagar, G. Marzari, H. Han, L. Badia-Bou, S. Gimenez, F. Fabregat-Santiago, I. Mora-Sero, J. Bisquert, U. Paik, Y.S. Kang, Adv. Energy Mater. 3 (2013) 176–182.
[19] R. Trevisan, P. Rodenas, V. Gonzalez-Pedro, C. Sima, R.S. Sanchez, E.M. Barea, I. Mora-Sero, F. Fabregat-Santiago, S. Gimenez, J. Phys. Chem. Lett. 4 (2013) 141–146.
[20] Z. Han, F. Qiu, R. Eisenberg, P.L. Holland, T.D. Krauss, Science 338 (2012) 1321–1324.
[21] S. Kirchmeyer, K.J. Reuter, Mater. Chem. 15 (2005) 2338–2339.
[22] S. Nagarajan, P. Sudhagar, V. Raman, K.S. Dhathathreyan, J. Yong Soo Kang, Mater. Chem. A 1 (2013) 1048–1054.
[23] B. Winther-Jensen, D.R. MacFarlane, Energy Environ. Sci. 4 (2011) 2790.
[24] C.H. Chang, Y.L. Lee, Appl. Phys. Lett. 91 (2007) 53503-1, 53503-3.
[25] M.K. Nazeeruddin, A. Kay, Rodicio, R. Humpbry-Baker, E. Miiller, P. Liska, N. Vlachopoulos, M. Gratzel, J. Am. Chem. Soc. 115 (1993) 6382–6390.
[26] D. Kowalski, S.P. Albua, P. Schmuki, RSC Adv. 3 (2013) 2154–2157.
[27] H. Mao, X.C. Liu, D.M. Chao, L.L. Cui, Y.X. Li, W.J. Zhang, C. Wang, J. Mater. Chem. 20 (2010) 10277–10284.
[28] S.V. Selvaganesh, J. Mathiyarasu, K.L.N. Phani, V. Yegnaraman, Nanoscale Res. Lett. 2 (2007) 546–549.
[29] C.-W. Kung, Y.-H. Cheng, H.-W. Chen, R. Vittal, K.-C. Ho, J. Mater. Chem. A1 (2013) 10693–10702.
[30] Jae Young Kim, Ganesan Magesh, Duck Hyun Youn, Ji-Wook Jang, Jun Kubota, Kazunari Domen, Jae Sung Lee Sci Rep., 3, (2013), 2681–1-2681–8.
[31] F. Zhang, M. Ceder, O. Inganäs, Adv. Mater. 19 (2007) 1835–1838.
[32] J. Bisquert, F. Fabregat-Santiago, I.N. Mora-Sero, G. Garcia-Belmonte, S. Gimenez, J. Phys. Chem. C 113 (2009) 17278–17290.
[33] A. Zaban, M. Greenshtein, J. Bisquert, Chem. Phys. Chem. 4 (2003) 859–864.
[34] I. Robel, V. Subramanian, M. Kuno, P.V. Kamat, J. Am. Chem. Soc. 128 (2006) 2385–2593.
[35] J.S. Luo, L. Ma, T.C. He, C.F. Ng, S.J. Wang, H.D. Sun, H.J. Fan, J. Phys. Chem. C 116 (2012) 11956–11963.
[36] H. Kim, K. Yong, ACS Appl. Mater. Interfaces 5 (2013) 13258–13264.
[37] S. Emin, M. Fanetti, F.F. Abdi, D. Lisjak, M. Valant, R. van de Krol, B. Dam, ACS Appl. Mater. Interfaces 5 (2013) 1113–1121.
[38] Y. Wang, J. Phys. Conf. Ser. 152 (2009) 012023.
[39] A.J. Bard, M.A. Fox, Acc. Chem. Res. 28 (1995) 141–145.
[40] Z.B. Chen, T.F. Jaramillo, T.G. Deutsch, A. Kleiman-Shwarsctein, A.J. Forman, N. Gaillard, R. Garland, K. Takanabe, C. Heske, M. Sunkara, E.W. McFarland, K. Domen, E.L. Miller, J.A. Turner, H.N. Dinh, J. Mater. Res. 25 (2010) 3–16.
[41] K. Maeda, K. Teramura, T. Takata, M. Hara, N. Saito, K. Toda, Y. Inoue, H. Kobayashi, K. Domen, J. Phys. Chem. B 109 (2005) 20504–20510.
[42] X.B. Chen, S.H. Shen, L.J. Guo, S.S. Mao, Chem. Rev. 110 (2010) 6503–6650.
[43] A. Thibert, F.A. Frame, E. Busby, M.A. Holmes, F.E. Osterloh, D.S. Larsen, J. Phys. Chem. Lett. 2 (2011) 2688–2694.